

# A Point Mass Proposal Method for Bayesian State-Space Model Fitting

Mary Llewellyn, Ruth King, Víctor Elvira and Gordon Ross

*School of Mathematics and Maxwell Institute for Mathematical Sciences,*

*University of Edinburgh, Edinburgh, UK*

January 2023

## Abstract

State-space models (SSMs) are often used to model time series data where the observations depend on an unobserved latent process. However, inference on the process parameters of an SSM can be challenging, especially when the likelihood of the data given the parameters is not available in closed-form. We focus on the problem of model fitting within a Bayesian framework, for which existing approaches include Markov chain Monte Carlo (MCMC) using Bayesian data augmentation, sequential Monte Carlo approximation, and particle MCMC algorithms, which combine sequential Monte Carlo approximations and MCMC steps. However, these different methods can be inefficient when sample impoverishment occurs during the sequential Monte Carlo approximation and/or when the MCMC algorithm mixes poorly. We propose the use of deterministic hidden Markov models (HMMs) to provide an efficient MCMC with data augmentation approach, imputing the latent states within the algorithm. Our approach deterministically approximates the SSM by a discrete HMM, which is subsequently used as an MCMC proposal distribution for the latent states in Metropolis-within-Gibbs steps. We demonstrate that the algorithm provides an efficient alternative method for state-space models with near-chaotic behaviour.

## 1 Introduction

State-space models (SSMs) describe time series observations as dependent on an unobserved system process (Durbin and Koopman, 2012). The unobserved system process of an SSM consists of a sequence of continuously-valued latent states that evolve through time but are not observed directly. Instead, observations are modelled as a function of these unobserved latent states via the observation process. SSMs have been applied to various problems, including the modelling of inflation rates (Koopman and Bos, 2004), neuron responses (Smith and Brown, 2003; Lin et al., 2019), animal movement (Patterson et al., 2008; Auger-Méthé et al., 2016), and population dynamics (Buckland et al., 2004; King, 2012; Newman et al., 2014).

Fitting an SSM usually refers to inference on the model parameters given the observations. However, outside of the discrete-state hidden Markov model (HMM) case (Rabiner, 1989), or special continuous cases, for example, linear Gaussian SSMs (Kalman, 1960; Durbin and Koopman, 2012), a closed-form expression for the likelihood does not exist, leading to model fitting challenges. The various approaches to approximating the likelihood include the use of linear Gaussian approximations (Julier and Uhlmann, 1997; Wan and Van Der Merwe, 2000), numerical methods using Laplace or HMM approximations (Bucy and Senne, 1971; Koyama et al., 2010; Langrock and King, 2013; Thygesen et al., 2017; Herliansyah et al., 2022), the use of sequential Monte Carlo to obtain an unbiased approximation to the likelihood (Beaumont, 2003; Andrieu and Roberts, 2009; Kantas et al., 2015; Deligiannidis et al., 2018), and Bayesian data augmentation approaches (Frühwirth-Schnatter, 2004; Fearnhead, 2011; Borowska and King, 2023). A review of these methods, and others, is given in Newman et al. (2022).

Here, we focus on Bayesian data augmentation approaches, which can be applied to general SSMs by specifying the latent states as additional auxiliary variables. In doing so, the data augmentation approach forms the joint posterior distribution of the model parameters and additional latent states (Tanner and Wong, 1987; Hobert, 2011). The resulting joint (complete data) likelihood of the parameters and states is typically available in closed-form, permitting the application of standard MCMC algorithms, such as the Gibbs sampler, Metropolis-Hastings algorithms, or Metropolis-within-Gibbs algorithms. An estimate of the marginal posterior distribution of the model parameters can then be obtained by simply retaining the sampled parameter values and disregarding the latent state samples to effectively marginalise over the states. It is, however, typically challenging to efficiently sample the latent state vector within an Metropolis-Hastings algorithm, since there are typically many highly correlated latent states, leading to poor mixing (Frühwirth-Schnatter, 2004). Updating the states one at a time typically performs very poorly due to the high correlation between states (Fearnhead, 2011), whilst designing good block-update proposal distributions can be challenging (Shephard and Pitt, 1997).

Historically, data augmentation has been combined with numerical approximation, sequential Monte Carlo, and/or MCMC to fit the parameters of an SSM. When an SSM is well-approximated by Gaussian distributions, efficient proposal distributions for the latent states in a data augmentation approach include those derived from Laplace approximation (Kristensen et al., 2016) and extensions to the Kalman filter (Giordani and Kohn, 2010). In the general case, more computationally intensive methods are usually required, such as the particle Gibbs (PG) sampler (Lindsten et al., 2012; Chopin and Singh, 2015; Fearnhead and Meligkotsidou, 2016) or particle Gibbs with ancestor sampling (PGAS) (Lindsten et al., 2014). PG and PGAS are classes of particle MCMC method (Andrieu et al., 2010) which use sequential Monte Carlo (SMC) to update all states simultaneously conditional on the parameters. In their use of SMC, PG and PGAS methods rely on few assumptions about the underlying state and observation distributions. However, these methods can be computationally expensive, particularly if many samples are required in the SMC steps due to sample impoverishment (Rainforth et al., 2016; Wang et al., 2017). One approach to over-

coming sample impoverishment is the introduction of deterministic resampling, which uses a deterministic grid over the state-space to retain samples that may otherwise be discarded in the SMC steps (Li et al., 2012). Although we do not develop a particle MCMC approach here, the use of a deterministic grid to efficiently sample the latent states is related to the approach presented in this paper.

We update the model parameters conditional on the imputed latent states, and we update the latent states conditional on the model parameters in Metropolis-within-Gibbs steps. We focus on the latter and propose the *point mass proposal Metropolis-Hastings* (PMPMH) algorithm, formulating proposals for the latent states in two steps. The first step uses a discretization of the state space into a set of pre-defined intervals (a grid) to reduce the SSM to an HMM. We then sample a sequence of intervals from the approximate distribution of the states given the model parameters, using forward-filtering backward-sampling (FFBS) algorithm (Rabiner, 1989). In the second stage of the algorithm, we then correct the discretization error imposed by the approximate HMM by sampling from within the intervals using a continuous proposal distribution, using these samples to update blocks of states in Metropolis-Hastings steps. The model parameters are updated conditionally on the latent states using standard Gibbs or Metropolis-within-Gibbs updates. The first step of the proposed algorithm is related to point mass smoothing (Bucy and Senne, 1971; Kitagawa, 1987; de Valpine and Hastings, 2002; Langrock et al., 2012; Langrock and King, 2013) and embedded HMMs (Neal, 2003; Shestopaloff and Neal, 2013; Finke et al., 2016; Shestopaloff and Neal, 2018), which use the tractable discrete case of an SSM, an HMM, to sample latent states. However, here we use the embedding of an HMM via deterministic grid cells to ensure latent states are proposed with reasonable posterior mass.

The rest of the paper is structured as follows. We start by defining SSMs and HMMs, and model fitting procedures for SSMs via Bayesian data augmentation in Section 2. We describe the proposed data augmentation scheme in Section 3, the PMPMH algorithm, in which we use a grid-based HMM approximation within a proposal distribution for the latent states. In Section 4, we provide three particular cases of the algorithm, each given by a different method for defining the grid cells, and describe when each can be usefully applied. Finally, we illustrate our approach with two case studies in Section 5 and discussed the proposed algorithm and extensions in Section 6.

## 2 State-space model inference

Here we define state-space models, the notation used throughout the paper, and the special case of discrete-valued system processes: HMMs. We then discuss the challenges of fitting state-space models to data and computational approaches in Section 2.1, motivating our proposed data augmentation algorithm.

We consider time series data observed at discrete (regular) time points up to time  $T$ ,  $y_{1:T} = (y_1, \dots, y_T)$ . An SSM models these data via (i) a system process of unobserved (latent) states,  $x_{1:T} = (x_1, \dots, x_T)$ ; and (ii) an observation process linking the latent process with the observed  $y_{1:T}$ . We allow the states to be continuous, taking values in some set

$x_t \in \chi$  for each  $t$ , and describe their evolution using initial state and transition distributions. Similarly, the observation process is described using an observed state distribution. As standard, we assume a first-order Markov process for the system process and that the observed data are conditionally independent given the underlying latent states, that is, the observation process is only a function of the latent state at time  $t$ . Given the set of model parameters, collectively denoted by  $\boldsymbol{\theta}$ , the SSM can be described mathematically by

$$\begin{aligned} \text{Initial state distribution:} & \quad p(x_1 \mid \boldsymbol{\theta}), \\ \text{State transition distribution:} & \quad p(x_t \mid x_{t-1}, \boldsymbol{\theta}), \quad t = 2, \dots, T, \\ \text{Observed state distribution:} & \quad p(y_t \mid x_t, \boldsymbol{\theta}), \quad t = 1, \dots, T. \end{aligned}$$

A particular case of an SSM is an HMM, in which the state space is discrete and finite. In other words, the states at time  $t$ ,  $x_t$ , take values in the set  $\{1, \dots, N\}$ . Therefore, when the SSM considered is an HMM, we simply re-define the initial state and transition probabilities for  $k, n = 1, \dots, N$  as

$$\begin{aligned} \text{Initial state probabilities:} & \quad P(x_1 = n \mid \boldsymbol{\theta}), \\ \text{State transition probabilities:} & \quad P(x_t = n \mid x_{t-1} = k, \boldsymbol{\theta}), \quad t = 2, \dots, T. \end{aligned}$$

## 2.1 Model fitting

We assume that we are primarily interested in inference on the model parameters,  $\boldsymbol{\theta}$ , although this may also extend to the latent states,  $x_{1:T}$ , depending on the application. In general, inference on the posterior distribution for  $\boldsymbol{\theta}$  requires a closed-form expression for the observed data (or marginal) likelihood,  $p(y_{1:T} \mid \boldsymbol{\theta})$ . The joint likelihood of the model parameters and latent states is given by

$$p(x_{1:T}, y_{1:T} \mid \boldsymbol{\theta}) = p(x_1 \mid \boldsymbol{\theta}) \prod_{t=2}^T p(x_t \mid x_{t-1}, \boldsymbol{\theta}) \prod_{t=1}^T p(y_t \mid x_t, \boldsymbol{\theta}). \quad (1)$$

A closed-form expression for the marginal likelihood typically only exists in the linear Gaussian case, where  $p(y_{1:T} \mid \boldsymbol{\theta})$  can be calculated using the Kalman filter (Kalman, 1960; Durbin and Koopman, 2012), or when the state space is discrete and finite (an HMM), where the marginalisation of Equation (1) amounts to summation over the state space (Rabiner, 1989). In general, however, the marginal likelihood is intractable for continuous SSMs, and standard MCMC implementations cannot be used. One solution is to use pseudo-marginal likelihood methods (Beaumont, 2003; Andrieu and Roberts, 2009), replacing the marginal likelihood with an unbiased estimate to formulate a valid Metropolis-Hastings approach, but we do not focus on these here.

Instead, we consider a Bayesian data augmentation approach. In this case, we form the joint posterior distribution over the model parameters and latent states (Tanner and Wong, 1987; Hobert, 2011),  $p(x_{1:T}, \boldsymbol{\theta} \mid y_{1:T}) \propto p(\boldsymbol{\theta})p(x_{1:T}, y_{1:T} \mid \boldsymbol{\theta})$ , thus using the joint

likelihood in Equation (1) directly. Since, in general, a closed-form expression exists for the joint likelihood term up to proportionality, the proportional likelihood can be evaluated, and standard MCMC approaches can be used targeting  $p(x_{1:T}, \boldsymbol{\theta} \mid y_{1:T})$ . Samples from the (marginal) posterior distribution of the parameters,  $p(\boldsymbol{\theta} \mid y_{1:T})$ , are then obtained by disregarding the state samples and retaining the parameter samples.

In order to sample from  $p(x_{1:T}, \boldsymbol{\theta} \mid y_{1:T})$ , a common approach is to sample the latent states and parameters in turn via their conditional distributions, simplifying the parameter updates (Carter and Kohn, 1994; Frühwirth-Schnatter, 2004; Durbin and Koopman, 2012). A Metropolis-within-Gibbs algorithm can be applied to target the joint distribution: in each iteration, we update the latent states conditional on the model parameters; and the model parameters conditional on the latent states (for which we now have a closed conditional likelihood expression). However, designing an efficient proposal distribution for the underlying state vector can be challenging. Ideally, we would be able to design a proposal distribution to update all states simultaneously and minimise the correlation between consecutive samples. In general, this state distribution is intractable, and designing an efficient approximation to the state distribution can be challenging since it is often high-dimensional in the number of temporal states. One approach updates all states simultaneously using a particle Gibbs algorithm (Chopin and Singh, 2015; Murphy and Godsill, 2016; Lindsten et al., 2014); values for the entire state vector are proposed at each iteration from a conditional sequential Monte Carlo algorithm. In this approach, proposed values for the entire state vector are always accepted and samples from the correct posterior distribution can be obtained. However, particle Gibbs methods can suffer from poor mixing sample impoverishment: degenerating particles being disregarded upon resampling, impacting mixing and convergence (Wang et al., 2017; Rainforth et al., 2016). Instead of updating all states simultaneously, for example via particle Gibbs updates, an alternative approach is to use a single-update algorithm: updating each latent state individually to reduce the required dimension of the proposal distribution, but this approach typically leads to very poor mixing due to correlation in the state process (Fearnhead, 2011; King, 2011).

A compromise between single and global updates of the latent states is to use block updates, simultaneously updating  $\ell$  consecutive states (Shephard and Pitt, 1997). The posterior conditional distribution of the states in a given block is, generally, of non-standard form, thus it can be challenging to define an efficient proposal distribution that accounts for the correlation between the states. We propose the use of the discrete analogy to SSMs, HMMs, to define an informative and efficient proposal distributions for blocks of latent states.

### 3 Point mass proposal Metropolis-Hastings

In this section, we propose the *point mass proposal Metropolis-Hastings* (PMPMH) algorithm. The setting is a Metropolis-within-Gibbs algorithm for data augmentation. The model parameters,  $\theta$ , are updated conditionally on  $x_{1:T}$  using a standard Metropolis-Hastings or Gibbs update, and we propose the PMPMH algorithm to sample Metropolis-Hastings proposals for the latent states given the model parameters.

Step 1 of the algorithm initially converts the SSM into an approximate HMM by discretizing the state-space at each time point, forming a deterministic grid. Grid cells are then sampled from the associated (discretized) posterior distribution, conditional on the model parameters, using the standard forward-filtering backward-sampling (FFBS) algorithm for HMMs (Rabiner, 1989) at a computational cost of  $\mathcal{O}(NT)$  for  $N$  grid cells at each time point. Given the sampled grid cells, Step 2 proposes values for  $x_{1:T}$  from within the cells using some specified (bounded) continuous proposal distribution.

For pedagogical purposes, we make a few assumptions in our initial description of the algorithm, for example, we derive the algorithm for one-dimensional state-spaces. Extensions to higher-dimensional state-spaces are possible, and we demonstrate the algorithm in the two-dimensional case with an example in Section 5. However, we note that there may be practically increased computational demands for higher-dimensional state-spaces. For notational simplicity, we present the algorithm for SSMs where the state-space and the number of grid cells are the same for each time point, that is, the state-space at all time points is denoted by  $\chi$ . However, the generalisation to state-spaces that vary over time is immediate by adapting the notation. Finally, we initially describe the algorithm in terms of updating the full set of latent states, with a version of the algorithm for block updates of the states described later.

#### 3.1 Step 1: sampling a grid cell trajectory

In this initial step, we formulate a discrete HMM approximation to the SSM and sample a trajectory, i.e., a value for  $x_{1:T}$ , from the discrete approximation. We then correct for the approximate sampling distribution using a Metropolis-Hastings step targeting the correct posterior distribution. First, we propose a partition of the whole state space into a grid: in the simplest case considered here, the state space at each time  $t$ ,  $\chi$ , is partitioned into intervals, forming grid cells. The  $N$  grid cells at time  $t$  are denoted  $I_t(n)$ ,  $n = 1, \dots, N$  and span  $\chi$  with no overlap. The respective outer grid cells have infinite length if the state space is unbounded. An example of such a partition is shown in Figure 1.

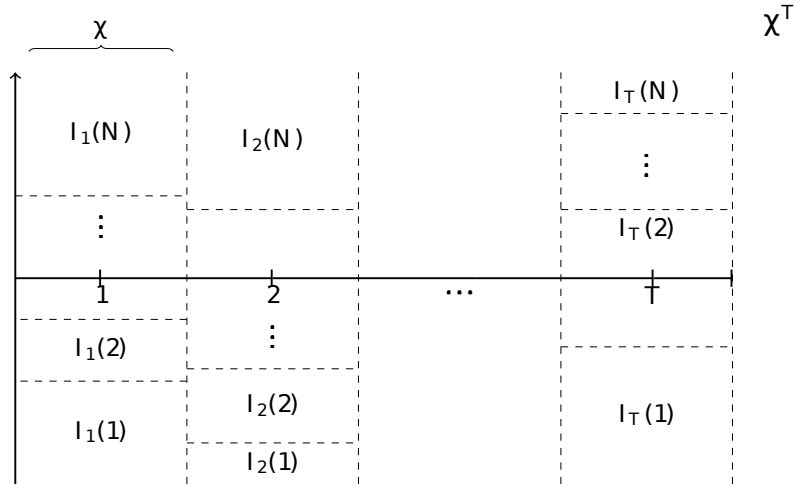


Figure 1: Example partition of a state space  $\chi^T$  for each time  $t$ . Each grid cell is labelled by the interval it covers.

The grid cells discretize the state space. Thus, the grid cell indices are the discrete states of an HMM. For the grid cells given by  $\{I_t(1), \dots, I_t(N)\}$ , the indices are simply  $\{1, \dots, N\}$ , with dynamics given by the SSM density of each grid cell. Mathematically, let  $B_t$  denote the random variable of the grid cell indices under the specified grid cell boundaries so that  $B_t \in \{1, \dots, N\}$  for  $t = 1, \dots, T$ . Then the HMM probabilities are given for states  $k, n \in \{1, \dots, N\}$  as

$$\begin{aligned}
 \text{Initial state probabilities:} & \quad P(B_1 = n \mid \boldsymbol{\theta}), \\
 \text{State transition probabilities:} & \quad P(B_t = n \mid B_{t-1} = k, \boldsymbol{\theta}), \quad t = 2, \dots, T, \\
 \text{Observed state distribution:} & \quad p(y_t \mid B_t = n, \boldsymbol{\theta}), \quad t = 1, \dots, T.
 \end{aligned}$$

These HMM probabilities are therefore, in general, defined by analytically intractable integrals of the state space equations over the given intervals:

$$\begin{aligned}
 P(B_1 = n \mid \boldsymbol{\theta}) &= \int_{I_1(n)} p(x_1 \mid \boldsymbol{\theta}) dx_1, \\
 P(B_t = n \mid B_{t-1} = k, \boldsymbol{\theta}) &= \int_{I_t(n)} \int_{I_{t-1}(k)} p(x_t \mid x_{t-1}, \boldsymbol{\theta}) dx_{t-1} dx_t, \quad 2 \leq t \leq T, \\
 p(y_t \mid B_t = n, \boldsymbol{\theta}) &= \int_{I_t(n)} p(y_t \mid x_t, \boldsymbol{\theta}) dx_t, \quad 1 \leq t \leq T.
 \end{aligned} \tag{2}$$

We approximate these integrals using simple (fast) deterministic methods, for example, the midpoint rule or other Riemann sum methods. Mathematically, we define  $L_t(n)$  as the length of the interval  $I_t(n)$ , with the length of any infinite grid cells set at some arbitrary (finite) length (discussed further in Appendix B). Within each grid cell, we choose a set of node points,  $\{\xi_t^s(n)\}_{s=1}^S$ . The set of nodes is defined *a priori* and is used to approximate the density functions across each grid cell by a polynomial. In the simple case where  $S = 1$



(that is, one node in each grid cell such as the mid-point), we have that  $\{\xi_t^s(n)\}_{s=1}^S = \xi_t(n)$ , and the HMM probabilities in Equations (2) for grid cells indices  $k, n = 1, \dots, N$  are approximated by

$$\begin{aligned}\hat{P}(B_1 = n \mid \boldsymbol{\theta}) &\propto L_1(n)p(\xi_1(n) \mid \boldsymbol{\theta}), \\ \hat{P}(B_t = n \mid B_{t-1} = k, \boldsymbol{\theta}) &\propto L_t(n)L_{t-1}(k)p(\xi_t(n) \mid \xi_{t-1}(k), \boldsymbol{\theta}), \quad t = 2, \dots, T, \\ \hat{P}(y_t \mid B_t = n, \boldsymbol{\theta}) &\propto L_t(n)p(y_t \mid \xi_t(n), \boldsymbol{\theta}), \quad t = 1, \dots, T,\end{aligned}$$

each appropriately normalised so that they sum to one and are thus valid probability mass functions. Once the probability mass function approximations have been obtained, grid cell indices are proposed from

$$\hat{P}(B_{1:T} \mid y_{1:T}, \boldsymbol{\theta}) \propto \hat{P}(B_1 \mid \boldsymbol{\theta}) \hat{P}(y_1 \mid B_1, \boldsymbol{\theta}) \prod_{t=2}^T \hat{P}(B_t \mid B_{t-1}, \boldsymbol{\theta}) \hat{P}(y_t \mid B_t, \boldsymbol{\theta}).$$

We sample indices from this distribution, denoted  $b'_{1:T}$ , using the forward-filtering backward-sampling (FFBS) algorithm in [Rabiner \(1989\)](#).

### 3.2 Step 2: sampling a point trajectory

Step 2 proposes continuous values for the states which will be subsequently corrected in Metropolis-Hastings steps. Given the discrete grid cell indices sampled previously, we propose values for  $x_{1:T}$  conditional on the corresponding intervals  $\{I_1(b'_1), \dots, I_T(b'_T)\}$ . This amounts to sampling  $x_{1:T}$  from the domain  $I_1(b'_1) \times I_2(b'_2) \times \dots \times I_T(b'_T)$ . For simplicity, we consider proposal distributions for each  $x_t$  independently and independently of  $\boldsymbol{\theta}$ , giving proposal distributions of the form  $q(x_t \mid x_t \in I_t(b'_t)) = q(x_t \mid B_t = b'_t)$ , for  $t = 1, \dots, T$ . For example, a natural choice is to propose each  $x_t$  from a uniform proposal distribution over  $I_t(b'_t)$  for finite  $I_t(b'_t)$ , or a truncated Gaussian distribution if  $I_t(b'_t)$  has infinite length. However, any distribution with domain  $I_t(b'_t)$  is applicable.

### 3.3 The PMPMH proposal distribution

The process of sampling a grid cell trajectory and sampling a value for  $x_{1:T}$  defines an independent proposal distribution on  $\chi^T$ . The density function of the proposed trajectories is therefore the probability of selecting the grid cell indices from a specified set of grid cell boundaries, combined with the density of the (continuous) values within those grid cells. Let  $B_{1:T}$  denote the random variables of the grid cell indices under the proposed grid, which may change across iterations with intervals  $I_t(n)$ ,  $n = 1, \dots, N$ ,  $t = 1, \dots, T$ . Then the density of the subsequently proposed state values,  $x'_{1:T}$ , is given by

$$q(x'_{1:T} \mid y_{1:T}, \boldsymbol{\theta}) = \hat{P}(B_{1:T} = b'_{1:T} \mid y_{1:T}, \boldsymbol{\theta}) \prod_{t=1}^T q(x'_t \mid B_t = b'_t). \quad (3)$$



The resulting proposed trajectory,  $x'_{1:T}$ , is retained according to the Metropolis-Hastings acceptance probability, given by

$$p(x_{1:T}, x'_{1:T} | \boldsymbol{\theta}) = \min \left( 1, \frac{p(x'_{1:T} | y_{1:T}, \boldsymbol{\theta}) q(x_{1:T} | y_{1:T}, \boldsymbol{\theta})}{p(x_{1:T} | y_{1:T}, \boldsymbol{\theta}) q(x'_{1:T} | y_{1:T}, \boldsymbol{\theta})} \right), \quad (4)$$

where  $p(x_{1:T} | y_{1:T}, \boldsymbol{\theta})$  denotes the posterior conditional distribution of  $x_{1:T}$  given  $y_{1:T}$  and  $\boldsymbol{\theta}$ ,  $q(x'_{1:T} | y_{1:T}, \boldsymbol{\theta})$  is as in Equation (3), and  $q(x_{1:T} | y_{1:T}, \boldsymbol{\theta})$  uses the same definition for the grid cells, that is, their indices,  $b_{1:T}$ , are such that  $x_t \in I(b_t)$  for all  $t$ .

The PMPMH method for obtaining a sample of  $x_{1:T}$  conditional on  $\boldsymbol{\theta}$  is summarised in Algorithm 1. For completeness, we also include the updates of  $\boldsymbol{\theta}$  conditional on  $x_{1:T}$ , which can be updated using standard Metropolis-Hastings or Gibbs updates conditional on the current chain value of the states.

---

**Algorithm 1** PMPMH algorithm

---

**Input:** initial values  $x_{1:T}^{(0)}$ ,  $\boldsymbol{\theta}^{(0)}$  and a number of iterations  $M$ . A Gibbs or Metropolis-Hastings sampling scheme to update  $\boldsymbol{\theta}$  from  $p(\boldsymbol{\theta} | x_{1:T}, y_{1:T})$ .

```

for iterations  $m = 1, \dots, M$  do
  1: Update  $\boldsymbol{\theta}^{(m)}$  from  $p(\boldsymbol{\theta} | x_{1:T}^{(m-1)}, y_{1:T})$ 

  2: Define a grid with indices  $B_{1:T}$ 
  3: for  $t = 1, \dots, T$  do ▷ (Step 1)
  4:   for  $k = 1, \dots, N$  do
  5:     calculate  $\hat{P}(B_t = n | y_{1:t}, \boldsymbol{\theta}^{(m)})$ 
  6:   sample  $b'_T$  from  $\{n, \hat{P}(B_T = n | y_{1:T}, \boldsymbol{\theta}^{(m)})\}_{n=1}^N$ 
  7:   for  $t = T - 1, \dots, 1$  do
  8:     sample  $b'_t$  from  $\{n, \hat{P}(B_t = n | B_{t+1} = b'_{t+1}, y_{1:t}, \boldsymbol{\theta}^{(m)})\}_{n=1}^N$ 

  9: for  $t = 1, \dots, T$  do ▷ (Step 2)
  10:   sample  $x'_t$  from  $q(x_t | B_t = b'_t)$ 

  11: sample  $u \sim U(0, 1)$ 
  12: if  $u < p(x_{1:T}^{(m-1)}, x'_{1:T} | \boldsymbol{\theta})$  then ▷ Equation (4)
  13:    $x_{1:T}^{(m)} \leftarrow x'_{1:T}$ 
  14: else  $x_{1:T}^{(m)} \leftarrow x_{1:T}^{(m-1)}$ 

```

---

### 3.4 Block updates of the latent states

Updating all of the states simultaneously may be inefficient if there are many latent states. We can, instead, update the states in smaller blocks: for a block of  $\ell$  states starting at time  $t$ , we sample an  $x_{t:t+\ell-1}$  from a proposal distribution of the form  $q(x_{t:t+\ell-1} | x_{t-1}, x_{t+\ell}, y_{t:t+\ell-1}, \boldsymbol{\theta})$ .

A block PMPMH proposal distribution is given by a simple adaptation of the case where all states are updated simultaneously, conditioning on the current states at either side of the block;  $x_{t-1}$  and  $x_{t+\ell}$ . Therefore, in Step 1, we condition on the current grid cell indices,  $b_{t-1}$  and  $b_{t+\ell}$ , such that  $x_{t-1} \in I(b_{t-1})$  and  $x_{t+\ell} \in I(b_{t+\ell})$  under the current grid definition. We then use FFBS to sample proposed indices from the grid cells in the block. In Step 2, we simply define the proposal distribution, as before, for each latent state in the given block,  $q(x_s \mid B_s = b'_s)$ , for  $s = t, \dots, t + \ell - 1$ . The PMPMH algorithm for block updates is summarised in Appendix C.

## 4 Defining the grid cells

We have, so far, given a broad framework for using an approximate HMM as an Metropolis-Hastings proposal distribution. The method fundamentally relies on the use of a deterministic grid to discretize the state-space. There are, however, many different ways to define the grid cells (their size and location), possibly resulting in substantially different proposal distributions and computational costs. We see in Section 5 that the efficiency of the algorithm is highly dependent on the choice of grid cell definition and resulting proposal distribution. Since the optimal choice depends on the application, we provide the reader with three approaches for defining the grid cells and describe when each can be usefully (and efficiently) applied. We discuss the other practical decisions in Appendix B.

### 4.1 Approach 1: equal grid cells

The first approach sets all finite cells equally sized and the same across all time points, that is,  $I_t(n) = I_s(n)$  for all  $t, s = 1, \dots, T$  and  $n = 2, \dots, N - 1$  (assuming an infinite lower and upper bound on the latent states). We assume that these equally sized grid cells are centred around the mean of the data,  $\frac{1}{T} \sum_{t=1}^T y_t$ , spanning a range of the state-space denoted by  $\mathcal{S}$ , though this approach could be adapted by centring the grid cells around another function of the data.

If the model parameters do not vary with time, only one transition matrix needs to be calculated per MCMC iteration, or when the model parameters are updated. For a fixed number of grid cells, this approach has the lowest computational cost of the approaches considered. However, since the grid cells are the same for each time point, but the regions of high posterior density may change at each time point, the grid cells should cover a large range of the state-space in order to ensure coverage of these high-density regions and good mixing. This may require many grid cells and a greater computational cost if the high posterior regions of the SSM are highly non-uniform over time, and hence this approach is most efficient for SSMs with uniform such regions.

## 4.2 Approach 2: data-driven quantiles

If the high posterior density regions vary over time, a time-inhomogeneous approximation to the HMM transition matrix may be more efficient than the previous approach. Hence, we set grid cells in this approach using the observed data at each time point. In particular, in the implementations of this paper, we set the grid cell boundaries at the quantiles of one-dimensional Gaussian distributions centered around each observed data point. For each time point,  $t$ , we set the boundaries at the quantiles of  $X$  where  $X \sim N(y_t, \sigma_y^2)$ . The variance of the Gaussian distribution,  $\sigma_y^2$ , is set at a scalar value, or as a function of the current observation process variance within the MCMC iterations and can be used to control the range that the majority of the grid cells cover via pilot tuning. The resulting quantiles are simply rounded if integer values are required. Note that simple extensions to this approach may include using a different distribution to set the quantiles, provided that its domain is in the state-space.

When the model parameters are updated, a transition matrix needs to be recalculated for each time point. It is, however, possible to reduce the computational cost of this approach by using the same transition matrix across several time points, centring, for example, on a single data point or the mean of the corresponding sub-series. By using the observed data at each time point, we aim to approximately concentrate the grid cells in areas that are likely to have high posterior mass at each time point. This method may be most efficient if the observed data used in the centring is a good proxy to the underlying state process and its dependencies.

## 4.3 Approach 3: latent state quantiles

The previous approaches define the grid cells independently of the state process, which may result in slow mixing if the latent states of the SSM are highly correlated over time. Thus, here we set the grid cells using the current latent states in the MCMC iterations at each time  $t$ . Let  $x_t^{(m-1)}$  denote the current state in the MCMC iterations at time  $t$ , then similarly to the previous approach, we define the grid cell boundaries at the quantiles of a Gaussian distribution  $X$  for each  $t$ , where  $X \sim N(x_t^{(m-1)}, \sigma_x^2)$ . As with the previous approach, the variance of the Gaussian distribution used to define the grid cells,  $\sigma_x^2$ , controls the span of the finite cells. Again, this variance could be set, for example, as a fixed value (chosen via pilot-tuning), as a function of the current estimate of the system process variance, or as a function of the current state within the MCMC iterations. We note that setting the majority of the grid cells to cover a small range relative to the high posterior density ranges worked well in practice (see Section 5).

In this approach, the transition matrices need to be recalculated at each time point for every change in the model parameters but will typically require fewer grid cells than the other approaches to achieve good mixing.

In general, there is a trade-off between the extent to which the grid cells are *well-placed* and the associated computational expense. For example, equally-sized grid cells are computationally fast but may give lower acceptance probabilities if they give coarse approximations in high-density regions. Where equally-sized grid cells give a poor acceptance probabilities, for example, due to non-uniformity in high posterior regions over time, acceptance probabilities may be improved using one of the other approaches at a greater computational expense.

## 5 Numerical illustrations

We demonstrate the proposed point mass proposal Metropolis-Hastings (PMPMH) algorithm via two case studies. The first is an SSM with a simple one-dimensional Gaussian mixture state process, demonstrating how the algorithm can be implemented, and the properties of the algorithm when different practical decisions are made. We then show how a similar PMPMH implementation can be used to efficiently sample the latent states of a more challenging 2-dimensional population growth model that can display near-chaotic behaviour.

In each case study, we compare the performance of the algorithm to two particle Gibbs algorithms: the particle Gibbs (PG) sampler ([Chopin and Singh, 2015](#); [Murphy and Godsill, 2016](#)) and the particle Gibbs with ancestor sampling (PGAS) algorithm ([Lindsten et al., 2014](#)), both with multinomial resampling. The two methods are particle MCMC algorithms and, like the proposed algorithm, sample from the joint posterior distribution of the states and parameters by updating each in turn from their full conditional distributions. The PGAS algorithm, in particular, is a state-of-the-art method that often improves upon the mixing properties of the PG algorithm by reducing sample impoverishment ([Nonejad, 2015](#); [Meent et al., 2015](#); [Kantas et al., 2015](#)), though at an increased computational cost. The code used to implement the PG, PGAS and PMPMH algorithms in each numerical illustration is given in Online Resource 1 of the Supplementary Information.

## 5.1 Gaussian mixture state-space model

We consider a simple one-dimensional Gaussian mixture state process:

$$\begin{aligned} x_1 &\sim w_1 N(1, \sigma_{\eta_1}^2) + (1 - w_1) N(1, \sigma_{\eta_2}^2), \\ x_t | x_{t-1} &\sim w_t N(x_{t-1}, \sigma_{\eta_1}^2) + \\ &\quad (1 - w_t) N(x_{t-1}, \sigma_{\eta_2}^2), \quad t = 2, \dots, T, \\ w_t &\sim \text{Bernoulli}(p), \quad t = 1, \dots, T, \end{aligned}$$

where  $p \in [0, 1]$  denotes the probability of selecting each mixture component of the state distribution (the Gaussian distributions with respective variances  $\sigma_{\eta_1}^2$  or  $\sigma_{\eta_2}^2$ ). Data,  $y_{1:T}$ , are observed according to  $y_t | x_t \sim N(x_t, \sigma_\epsilon^2)$  and the model parameters are given by  $\theta = (p, \sigma_{\eta_1}^2, \sigma_{\eta_2}^2, \sigma_\epsilon^2)$ . We simulate two data sets from this model,  $y_{1:600}^{(1)}$  using  $\theta = (0.9, 1, 700, 1)$  and  $T = 600$  (Model 1), and  $y_{1:1000}^{(2)}$  using  $\theta = (0.99, 1, 10000, 10)$  and  $T = 1000$  (Model 2), shown in Figure 2.

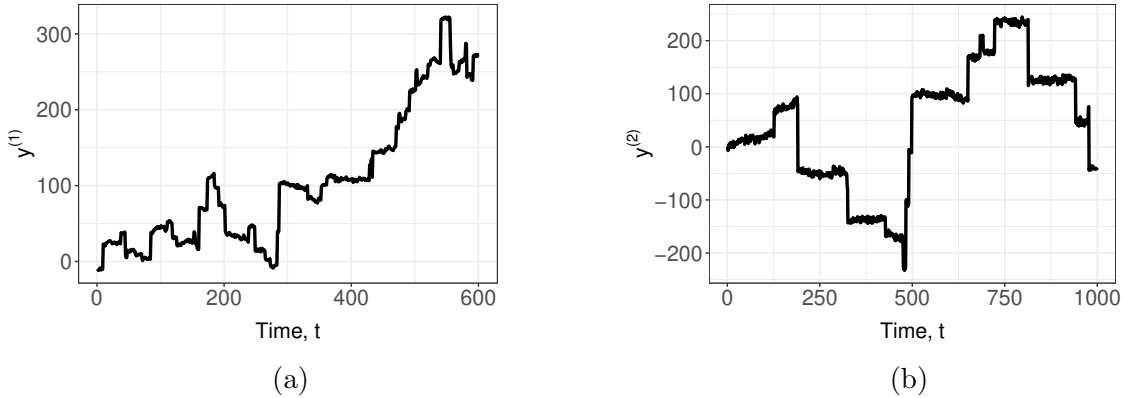


Figure 2: Simulated data from the Gaussian mixture SSM:  $y_{1:600}^{(1)}$  using (a)  $\theta = (0.9, 1, 700, 1)$ ,  $T = 600$ , and (b)  $y_{1:1000}^{(2)}$  using  $\theta = (0.99, 1, 10000, 10)$ ,  $T = 1000$ .

Both data sets are simulated with a high-variance second mixture component, selected with a low probability, resulting in infrequent but large *jumps* in the state process. The parameter values for Model 2 result in more occasional and larger jumps in the state process than the first. We compare the properties of the algorithm in both cases.

### 5.1.1 PMPMH implementation

We sample from the joint posterior distribution of the states and parameters, updating  $x_{1:T}$  and  $\theta$  from their conditional distributions. The sampling schemes and priors for updating  $\theta$  are given in Appendix A.1. Here, we apply the two stages of the PMPMH algorithm to update  $x_{1:T}$  conditional on  $\theta$ . The PMPMH framework presented can be adapted in a number of ways, for example, by changing the deterministic integration method used to approximate the HMM probabilities, the number of grid cells, and the distribution used

to propose values from within grid cells. However, we show in this section that we achieve stable and efficient performance by fixing a number of these decisions and opting for the simple choices given in Appendix B.

Instead, we focus on the practical decisions that are relevant to the efficiency of the algorithm: (a) the choice of each Approach 1 – 3 of Section 4 (including the range of the state-space covered by the finite grid cells,  $\mathcal{S}$ , which we set using scalar variances), (b) the number of grid cells,  $N$ , and (c) the temporal block sizes in which the states are updated,  $\ell$ . We test the efficiency of the algorithm under various combinations of these tuning parameters:

- (a) the finite grid cells in Approach 1 over a range of  $\mathcal{S} = 150, 250, 350, 450, 550$  units for both data sets (compared to the range of each set of observations,  $y_{1:600}^{(1)}$  and  $y_{1:1000}^{(2)}$ , equal to 334 and 478 units respectively). In Approaches 2 and 3, we use  $\mathcal{S} = 1, 3, 5, 7, 9, 11, 13, 15$  units for both models,
- (b)  $N = 5, 10, 20$ ,
- (c)  $\ell = 1, 4, 10$ , overlapping blocks by one state to improve the mixing of the states at the “boundaries” of each block as suggested in (Fearnhead, 2011).

### 5.1.2 Results

For each combination of the tuning parameters listed above, the results are based on 10 separate runs of 10,000 iterations each, taking 1.3–7.5 hours with 1.6 GHz CPU for Model 1 (depending on the number of grid cells and the approach chosen) and 2.2–11 hours for Model 2. We present the results for each model in Tables 1 and 2 respectively.

Increasing the number of grid cells,  $N$ , results in a more accurate approximation to  $p(x_{1:T} \mid y_{1:T}, \theta)$  in the region covered by the finite grid cells, improving mixing but at a higher computational cost. The equally-spaced grid cell Approach 1 performed poorly on both simulated models compared to the quantile-based methods of Approaches 2 and 3, requiring a large span for both models (350 and 550 units respectively) due to a large range of values in the high posterior regions, and thus large numbers of grid cells and a large computational cost, to provide a reasonable HMM approximation.

Under Approaches 2 and 3, using blocks of size  $\ell = 10$  or a span for the finite cells greater than 11 units required more than  $N = 20$  grid cells for convergence and resulted in much more costly and less efficient implementations than the other sets of tuning parameters. Further, using single-site updates ( $\ell = 1$ ) gave poor mixing when compared to blocks of size  $\ell = 4$  due to the correlation between consecutive states. The results when using  $\ell = 1, 10$ , a finite span greater than 11 units and  $N > 20$  are thus excluded from Tables 1 and 2 for brevity.

$y_{1:600}^{(1)}$						
N	$\mathcal{S}$	% of range of the data	Approach 2		Approach 3	
			ESS	ESS/s	ESS	ESS/s
5	1	0.3	100	0.02	-	-
	3	0.9	900	0.18	1000	0.20
	5	1.5	700	0.14	100	0.02
	7	2.1	300	0.06	-	-
	9	2.6	200	0.04	-	-
	$\geq 11$	$\geq 3.3$	-	-	-	-
10	1	0.3	100	0.01	-	-
	3	0.9	1000	0.10	1700	0.17
	5	1.5	2400	0.24	200	0.02
	7	2.1	2200	0.22	-	-
	9	2.6	2000	0.20	-	-
	$\geq 11$	$\geq 3.3$	-	-	-	-
20	1	0.3	100	0.00	-	-
	3	0.9	700	0.03	2200	0.08
	5	1.5	2700	0.10	1000	0.04
	7	2.1	3000	0.11	-	-
	9	2.6	3000	0.11	-	-
	$\geq 11$	$\geq 3.3$	-	-	-	-

Table 1: Average effective sample size (ESS) and effective sample size per second (ESS/s) for Approaches 2 and 3 of the PMPMH algorithm with temporal blocks of size  $\ell = 4$ . The span of the finite cells is denoted by  $\mathcal{S}$ , the number of grid cells,  $N$ . Dashed lines indicate that convergence had not occurred within 10,000 iterations. The ESS is rounded to the nearest 100 to account for variation between chains. Since at least one model parameter was updated at each iteration for each run of the algorithm, the computational times are the same for Approaches 2 and 3: 5,000 seconds for  $N = 5$ , 10,000 seconds for  $N = 10$ , and 27,000 seconds for  $N = 20$ , where the computational time is rounded to the nearest 1000 seconds to account for variations in computing speeds.

The results for Approaches 2 and 3 in Table 1 use blocks of size  $\ell = 4$ , and where convergent, converge within 1000 – 5000 iterations using the Brooks-Gelman-Rubin (BGR) diagnostics in Gelman and Rubin (1992); Brooks and Gelman (1998). In the implementations relating to Model 1, both approaches for defining the grid cell boundaries yield similar levels of efficiency when considering the effective sample size (ESS) per second, likely since the small observation error means that both approaches focus grid cells in roughly the same region of the state space around the current state. This is potentially also the reason that both methods required a small span for the finite cells and a small number of grid cells for convergence relative to the range of the data (1 – 9 vs. 344 units, around 0.3 – 2.6% of the range of the data): as is true of proposal distributions that make local moves, grid cells can be focused over a smaller range of the data compared to global-move approaches and still achieve good acceptance probabilities and mixing. The smaller range also means that as



$y_{1:1000}^{(2)}$						
N	$\mathcal{S}$	% of range of the data	Approach 2		Approach 3	
			ESS	ESS/s	ESS	ESS/s
5	$\leq 3$	$\leq 0.6$	-	-	-	-
	5	1	-	-	200	0.03
	7	1.5	-	-	500	0.06
	$\geq 9$	$\geq 1.9$	-	-	-	-
10	$\leq 3$	$\leq 0.6$	-	-	-	-
	5	1	-	-	200	0.02
	7	1.5	100	0.01	500	0.04
	9	1.9	200	0.02	200	0.02
20	11	2.3	100	0.01	-	-
	$\geq 13$	$\geq 2.7$	-	-	-	-
	$\leq 3$	$\leq 0.6$	-	-	-	-
	5	1	-	-	300	0.01
	7	1.5	100	0.00	600	0.02
	9	1.9	200	0.01	400	0.01
	11	2.3	200	0.01	400	0.01
	$\geq 13$	$\geq 2.7$	-	-	-	-

Table 2: Average effective sample size (ESS) and effective sample size per second (ESS/s) for Approaches 2 and 3 of the PMPMH algorithm with temporal blocks of size  $\ell = 4$ . The span of the finite cells is denoted by  $\mathcal{S}$ , the number of grid cells,  $N$ . Dashed lines indicate that convergence had not occurred within 10,000 iterations. The ESS is rounded to the nearest 100 to account for variation between chains. Since at least one model parameter was updated at each iteration for each run of the algorithm, the computational times are the same for Approaches 2 and 3: 8,000 seconds for  $N = 5$ , 13,000 seconds for  $N = 10$ , and 38,000 seconds for  $N = 20$ , where the computational time is rounded to the nearest 1000 seconds to account for variations in computing speeds.

few as 5 grid cells can be used to achieve good convergence properties (compared to 50 in Approach 1) via a good HMM approximation over the region, reducing the computational cost of the approaches.

In comparison to Model 2, where the observation process variance is larger, Approach 2 is different from a local-move proposal distribution and generally exhibits poor mixing and convergence in comparison to Approach 3. Conversely, the local moves of Approach 3 are effective at achieving convergence and exhibit relatively stable performance even for  $N = 5$ . The efficient ranges for the finite grid cells are similar to those in the implementations of the first model as a percentage of the range of the data (here, 1 – 2.3% of the range of the data).

We also fitted both of the models using the PG and PGAS algorithms with 5 to 1000 particles, and various combinations of resampling thresholds based on the standard percentage ESS criterion (Cappé et al., 2005). The PG sampler did not converge for either model using as many as 1000 particles, resulting in computational times of around 14 hours

for Model 1 and 28 hours for Model 2 on 1.6 GHz CPU. Conversely, the PGAS sampler converged using as few as 5 particles for both models. On the whole, the PGAS sampler gave greater levels of efficiency than the PMPMH algorithm for both of the models, achieving an average ESS per second of around 4.45 for Model 1 and 1.49 for Model 2. However, this efficiency was not uniform across all states. The average ESS per second of the states simulated according to the second mixture was 0.25 to 0.41 for Model 1 and 0.004 to 0.008 for Model 2. In contrast, where convergent, the PMPMH algorithm was more robust to the mixture associated with the state, with the ESS per second of states in the second mixture minimally 99% of those quoted in Tables 1 and 2 (the average ESS per second in the second mixture-distributed states ranging from 0.01 to 0.24 for Model 1 and 0.01 to 0.06 for Model 2). We now investigate the comparative performance of the algorithm on a model that can display near-chaotic behaviour.

## 5.2 Nicholson’s blowfly model

We consider Nicholson’s Blowfly model for chaotic population growth in Wood (2010). The population counts over time, denoted by  $N_{1:T}$ , arise from two correlated survival and birth processes, denoted  $S_{1:T}$  and  $R_{\tau+1:T}$ ,  $\tau > 0$ , respectively. Following Wood (2010), we let  $\exp(-\delta\epsilon_t)$  denote the daily survival probability with associated environmental error term  $\epsilon_t$ , such that  $\epsilon_t \sim \Gamma(\beta_\epsilon, \beta_\epsilon)$ ,  $\beta_\epsilon > 0$ . The survival component of the system process is given for  $t = 1, \dots, T$  by

$$S_t \sim \text{Binom}(N_{t-1}, \exp(-\delta\epsilon_t)),$$

Letting  $e_t$  denote an environmental noise term in the reproductive process such that  $e_t \sim \Gamma(\beta_e, \beta_e)$ ,  $\beta_e > 0$ , the reproductive component of the system process is given for  $t = \tau + 1, \dots, T$ , by

$$R_t \sim \text{Po} \left( P N_{t-\tau-1} \exp\left(-\frac{N_{t-\tau-1}}{N_0}\right) e_t \right),$$

where  $N_t = S_t + R_t$  for  $t = \tau + 1, \dots, T$  and  $N_t = S_t$  for  $t = 1, \dots, \tau$ . We let  $\tau = 5$  be the known time lag between population count and subsequent birth count, and  $N_0 = 50$  is the known initial population count. Further,  $\epsilon_{1:T}$  and  $e_{\tau+1:T}$  are known. The survival and birth processes,  $S_{1:T}$  and  $R_{\tau+1:T}$ , are unknown latent states, with observed population counts  $y_t \sim \text{Po}(\phi N_t)$ , for all  $t$ . Further, the model parameters  $\boldsymbol{\theta} = (\delta, P, \beta_\epsilon, \beta_e, \phi)$  are unknown and positively valued. Figure 3 shows the simulated data used in this case study,  $y_{1:T}$ , using  $\boldsymbol{\theta} = (0.7, 50, 1, 0.1, 1)$  and  $T = 300$ .

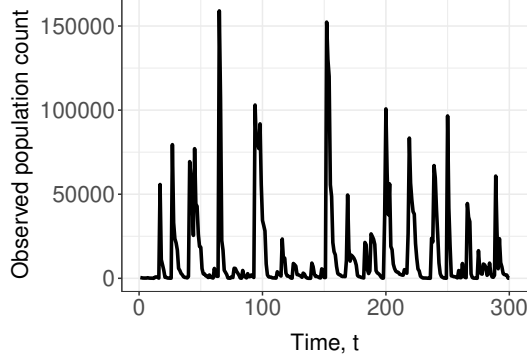


Figure 3: Simulated blowfly population count data using  $T = 300$  and  $\theta = (0.7, 50, 1, 0.1, 1)$ .

### 5.2.1 PMPMH implementation

We devise an Metropolis-Hastings scheme targeting the joint posterior distribution of the unknown latent states and model parameters,  $p(S_{1:T}, R_{\tau+1:T}, \theta \mid y_{1:T})$ . The model parameters are updated from their full conditional distribution,  $p(\theta \mid S_{1:T}, R_{\tau+1:T}, y_{1:T})$ , using the priors and sampling schemes given in Appendix A.2. In this section, we describe how the PMPMH algorithm can efficiently update the latent states,  $S_{1:T}$  and  $R_{\tau+1:T}$ , conditional on  $\theta$ .

First, the state process is now two-dimensional at each time point. In order to simplify the design of the grid used within the PMPMH algorithm, we build separate PMPMH proposal distributions targeting the full conditional distributions in each state dimension,  $p(S_{1:T} \mid R_{\tau+1:T}, y_{1:T}, \theta)$  and  $p(R_{\tau+1:T} \mid S_{1:T}, y_{1:T}, \theta)$ , respectively. To sample from each of the full conditional distributions in turn, a number of the practical decisions remain the same as in the previous example of Section 5.1. We first fix several of the practical decisions to those in Appendix B and use blocks of size  $\ell = 4$ , overlapping blocks by one state to reduce the correlation between states at the block boundaries. We test the performance of the algorithm for  $N \in \{10, 20, 50\}$  grid cells.

There are two main differences in this implementation compared to the previous example. The first accounts for the near-chaotic state processes and the large range of the data ( $1.59 \times 10^5$  units). We apply the current state-centred Approach 3 of Section 4, which requires fewer grid cells for good mixing properties due to the lower span for the finite cells required to achieve efficient (more local) moves. Within this approach, we permit large variability around large values for the state process by adjusting the variance of the Gaussian distributions used to set the boundaries of the grid cells: we set the variance proportional to the current state at each time point. We try factors of proportionality of 0.1, 0.25, 0.5, 1, with finite grid cells between the  $q$  and  $1 - q$  quantiles with  $q = 0.01, 0.1, 0.2$ , resulting in (average) spans for the finite cells ranging from  $\mathcal{S} = 52 - 400$ . The second difference is that we ensure the grid cells are over a discrete space bounded at zero by rounding the quantiles used to determine the grid cells, setting the lower boundary to zero if needed.

### 5.2.2 Results

We assessed the performance of the PMPMH algorithm using 10 independent MCMC simulations of 50,000 iterations and present the performance metrics in Table 3. Where the implementations of the PMPMH algorithm converged, convergence was achieved within 4,000 – 18,000 iterations, taking 11 – 27 hours using 1.6 GHz CPU. Fairly consistent and efficient performance (in terms of ESS per second, Table 3) is achieved using 20 – 50 grid cells with the finite cells covering a region of the state-space 0.05 – 0.25% of the range of the data ( $\mathcal{S} \in [82, 400]$ ).

Max N	Average S		ESS	ESS/s
	$\mathcal{S}$	$\mathcal{R}$		
10	$\leq 76$	$\leq 70$	-	-
	82-100	75-90	2500	0.05
	100-200	90-180	3200	0.07
	$> 200$	$> 180$	-	-
20	$\leq 76$	$\leq 70$	-	-
	82-100	75-90	4400	0.09
	100-200	90-180	5400	0.09
	200-300	180-260	7000	0.11
	300-400	260-300	6700	0.10
50	$\leq 76$	$\leq 70$	-	-
	82-100	75-90	4400	0.06
	100-200	90-180	5700	0.06
	200-300	180-260	7300	0.08
	300-400	260-300	6900	0.07

Table 3: Average ESS and ESS/s across state and parameter samples for various sets of tuning parameters under Approach 3 with blocks of size  $\ell = 4$ . Since the span of the finite cells varies across time points, we provide the average span provided by the MCMC output. The ESS has been rounded to the nearest 100 to account for the variability within the chains.

Approach 3 mixes effectively by producing a reasonable HMM approximation in a relatively small region around the current state and is also computationally cheap to implement. The efficiency of the algorithm reduces at an upper bound of 50 grid cells, indicating that the improved mixing properties of the algorithm are not justified by the extra cost when compared with using fewer grid cells. Conversely, 10 grid cells, although lower in computational cost, do not produce a sufficiently accurate approximation to the posterior in the region of the current state. We also note that, similarly to the previous case study, implementations relying on *extremely* small moves around the state space (finite cells  $< 0.05\%$  of the range of the data) gave poor mixing and convergence properties.

The PGAS sampler, when applied to the model using both joint updating of the latent states and updating each latent state process in turn from their full conditional distributions, did not converge in 50,000 iterations with 1000 particles, remaining in a range of the state space unrepresentative of the posterior due to sample impoverishment and taking 160 hours with 1.6 GHz CPU.

## 6 Discussion

We provide a novel approach for fitting general state-space models to observed data. The idea utilises tractable HMM approximations to efficiently update the unobserved latent states in an Metropolis-Hastings algorithm. We demonstrate the generality of the proposed approach by its application to two problems, including a near-chaotic problem that is generally challenging. The proposed PMPMH algorithm is demonstrated to provide reliable posterior estimates within reasonable computational time frames and compared to the PGAS algorithm often applied to such problems. The flexibility of the PMPMH approach via the tuning parameters, including the location, size, and number of grid cells, provides an adaptable and efficient algorithm. Using simple methods for placing the grid cells, such as equally-sized grid cells, can be efficient since they are computationally cheap. However, such simple methods may require a large number of grid cells to achieve good mixing if the range of the data is large. A current state-centered approach for approximating the HMM is useful, especially when the state space covers a large range, and using a data-centered approach is useful provided the range of the data is small.

The PMPMH approach presents some interesting points for future research. One way to reduce the overall computational cost of the algorithm is to reduce the number of times the HMM approximation is calculated across iterations. This is valid for approximation methods that do not depend on the current state or model parameters. However, for deterministic grids that adapt to previous samples (for example, Approaches 2 and 3), the resulting posterior estimate may become biased since the chain is no longer Markovian (Haario et al., 1999). However, Haario et al. (1999) also show that the bias introduced is negligible in some applications and that unbiased samples can be obtained by introducing some pre-determined stopping criterion for updating the grid, that is, specifying a number of iterations beyond which the grid is no longer updated. The computational gains from updating the HMM approximation less frequently could, however, be balanced with potentially reduced mixing properties. For example, local-move grids using a low span for finite cells are more sensitive to the frequency of the HMM approximation since they rely on proposed moves being made in the region of the current state. However, updating the grid less frequently may give an efficient approach when applied to more global-move samplers.

One may also attempt to find efficient ways to adapt the HMM approximations. With any such adaptations, there is a trade-off between the improved mixing properties and the computational cost arising from the complexity of the method. For example, in Step 1 of the algorithm, more complex numerical integration methods could be used to approximate the SSM density in each grid cell. Such methods include increasing the number of points in each

grid cell used for approximation calculations, simple linear functions joining evaluations at midpoints, or other fast evaluations that include the gradient in each grid cell. There may also be ways to improve the efficiency of the within-cell proposal distributions in Step 2, including approaches that approximate the posterior density in each grid cell where the conditional posteriors are irregular or vary in an unsystematic way depending on the value of the parameter. These approaches could be valuable to explore for more complex SSMS, in which the improved mixing may justify the added computational cost. Further, these approaches to improving mixing in each step may permit the use of fewer grid cells, decreasing the overall computational cost, which may also permit greater scalability of the HMM to higher dimensional latent spaces. Although we demonstrated the scalability of the proposed algorithm to higher dimensional spaces by updating each state dimension conditionally on the remaining state dimensions, higher dimensional spaces are a particular challenge if individual state dimensions are highly correlated, resulting in poor mixing. This scalability of grid-based methods to higher dimensional spaces is a challenge to the proposed algorithm and an active area of research.

## Supplementary material

GitHub repository containing the R code for the implementations of the PMPMH, PG and PGAS algorithms in Section 5:

<https://github.com/mallewellyn/PMPMH>.

## Acknowledgements

Funding: M.L. was supported by studentship funding from the Engineering and Physical Sciences Research Council (EPSRC). R.K. was supported by the Leverhulme Research Fellowship RF-2019-299. V.E. was supported by the Leverhulme Research Fellowship RF-2021-593.

## Appendix A Parameter prior distributions

### Appendix A.1 Gaussian Mixture State-Space Model Parameters in Section 5.1

In Section 5.1, we conditionally update the parameters from both  $p(\boldsymbol{\theta} \mid x_{1:T}, y_{1:T}^{(1)})$  and  $p(\boldsymbol{\theta} \mid x_{1:T}, y_{1:T}^{(2)})$  using single-site conjugacy in the observation variance parameter. For both Model 1 and Model 2, we assign vague priors to enable comparison with the simulated parameter for diagnostic purposes. For Model 1,

$$\sigma_\epsilon^2 \sim \Gamma^{-1}(2, 2),$$

resulting in a Gibbs sampler for  $\sigma_\epsilon^2$ . We assign further high-variance priors to the other parameters in Model 1:

$$\begin{aligned} p &\sim U(0, 1), \\ \sigma_{\eta_1}^2 &\sim \Gamma^{-1}(2, 2), \\ \sigma_{\eta_2}^2 &\sim \Gamma^{-1}(2, 700), \end{aligned}$$

where  $p$ ,  $\sigma_{\eta_1}^2$  and  $\sigma_{\eta_2}^2$  are proposed at iteration  $m$  from uniformly-distributed random walk proposals over intervals of length 0.3, 2, and 160 units respectively. For Model 2, we similarly assign the independent priors:

$$\begin{aligned} \sigma_\epsilon^2 &\sim \Gamma^{-1}(2, 10), \\ p &\sim U(0, 1), \\ \sigma_{\eta_1}^2 &\sim \Gamma^{-1}(2, 2), \\ \sigma_{\eta_2}^2 &\sim \Gamma^{-1}(2, 700), \end{aligned}$$

where the prior for  $\sigma_\epsilon^2$  again results in Gibbs steps for this parameter. We propose  $p$ ,  $\sigma_{\eta_1}^2$  and  $\sigma_{\eta_2}^2$  at iteration  $m$  from a uniform random walk proposal distribution over 0.02, 0.5, and 20000 units respectively. All intervals for the random walk proposal distributions are set using pilot tuning.

## Appendix A.2 Nicholson's Blowfly Model Parameters in Section 5.2

We give details for the priors and sampling schemes for the model parameters,  $\theta$ , in Section 5.2. Once again, we make use of the conjugate priors for single site updates of  $\theta$  where possible and assign vague priors to help diagnose convergence:

$$\begin{aligned} \delta &\sim \Gamma(0.007, 0.01), \\ P &\sim \Gamma(50, 1), \\ \beta_\epsilon &\sim \Gamma^{-1}(100, 100), \\ \beta_e &\sim \Gamma^{-1}(10, 1), \\ \phi &\sim \Gamma(0.01, 0.01). \end{aligned}$$

This results in single-site Gibbs updates for  $P$  and  $\phi$ . For  $\delta$ ,  $\beta_\epsilon$  and  $\beta_e$  and we use a random walk Metropolis-Hastings step with uniform proposal distributions over intervals of length 0.03, 0.5, and 0.05 respectively. The parameters of the proposal distributions were chosen via pilot tuning.



## Appendix B Practical decisions

We make a number of practical decisions in order to implement the PMPMH algorithm in our case studies. We opt for simple choices for most of these and discuss these here.

### Appendix B.1 Deterministic integration method

In Section 3.1, we focus on the simple case for approximating the HMM probabilities in each grid cell: midpoint integration using  $S = 1$ . However, the Riemann sum integral approximation method scales simply for higher order polynomials where  $S \geq 2$ , or these methods can be easily replaced by more complex numerical integration strategies. However, the complexity of these methods should be balanced with their associated computational cost to ensure efficiency in this step. We therefore test the efficiency of the algorithm using midpoint integration ( $S = 1$ )

The *midpoint* and length of the cells must be defined to apply midpoint integration, even when the  $n = 1$  or  $n = N$  grid cells have an infinite range. In these infinite cells, we simply set this artificial length at the average length of the finite cells, and we set the artificial midpoint at half that length away from the corresponding upper or lower boundary of the finite cells. Further, to ensure that the HMM probabilities are sufficiently high to avoid the proposal distribution resulting in a ‘near-reducible’ Markov chain, we set a lower bound on the HMM probabilities. In all the implementations of this paper, we use a lower bound of 0.01 and renormalize so that they sum to one.

### Appendix B.2 Proposal distributions within the grid cells

Once we have sampled a set of grid cells, indexed by  $b'_{1:T}$  as per Section 3.2, we sample point values from within the grid cells using simple proposal distributions for each  $t \geq 1$ . In all implementations, we sample from uniform distributions with domain in the finite grid cells.

To sample values for the state in infinite grid cells in the first case study of Section 5.1, we sample from a truncated Gaussian distribution with mean equal to the finite boundary and a variance of 5. The variance of the infinite-cell distribution is relatively low so that proposals in this grid cell are mostly concentrated around the boundary of the finite cells, increasing the density in the tails of the proposal distribution. In the second case study, we sample from a Poisson distribution with mean parameter equal to 2 (again to ensure a relatively heavy-tailed proposal distribution), shifted to the lower bound of the upper (infinite) grid cell.

## Appendix C Pseudocode for the PMPMH algorithm with block updates

Here we present the pseudocode describing the two stages of the PMPMH algorithm with the states updated in blocks. This supplements the description of the block-updating procedure in Section 3.4.

Note that, in this case, the acceptance probability for a proposed set of  $\ell$  states starting at time  $t$ ,  $x'_{t:t+\ell-1}$ , is given by

$$\begin{aligned}
 p(x_{t:t+\ell-1}, x'_{t:t+\ell-1} \mid \boldsymbol{\theta}) = & \\
 & \frac{p(x'_{t:t+\ell-1} \mid x_{t-1}, x_{t+\ell}, y_{t:t+\ell-1}, \boldsymbol{\theta})}{p(x_{t:t+\ell-1} \mid x_{t-1}, x_{t+\ell}, y_{t:t+\ell-1}, \boldsymbol{\theta})} \times \\
 & \frac{q(x_{t:t+\ell-1} \mid x_{t-1}, x_{t+\ell}, y_{t:t+\ell-1}, \boldsymbol{\theta})}{q(x'_{t:t+\ell-1} \mid x_{t-1}, x_{t+\ell}, y_{t:t+\ell-1}, \boldsymbol{\theta})}
 \end{aligned} \tag{C.1}$$

where in the first block,  $p(x_{t:t+\ell-1} \mid x_{t-1}, x_{t+\ell}, y_{t:t+\ell-1}, \boldsymbol{\theta}) = p(x_{t:t+\ell-1} \mid x_{t+\ell}, y_{t:t+\ell-1}, \boldsymbol{\theta})$ , and similarly for the proposal density. Likewise, in the last block,  $p(x_{t:t+\ell-1} \mid x_{t-1}, x_{t+\ell}, y_{t:t+\ell-1}, \boldsymbol{\theta}) = p(x_{t:t+\ell-1} \mid x_{t-1}, y_{t:t+\ell-1}, \boldsymbol{\theta})$ .

---

**Algorithm 2** PMPMH algorithm: block updates

---

**Input:** initial values  $x_{1:T}^{(0)}$ ,  $\theta^{(0)}$ , a number of iterations  $M$ . A blocking strategy for the states: a block size  $\ell$  and a set of starting points for each block  $\{1, \dots, D\} \subset \{1, \dots, T\}$ . A Gibbs or Metropolis-Hastings sampling scheme to update  $\theta$  from  $p(\theta \mid x_{1:T}, y_{1:T})$ .

---

For  $1 \leq t \leq \ell$  (block  $d = 1$ ), define

$$\hat{P}(B_t = k \mid B_{d-1} = b_{d-1}, y_{d:t}, \theta) = \hat{P}(B_t = k \mid y_{d:t}, \theta),$$

$$\hat{P}(B_t = k \mid B_{d-1} = b_{d-1}, B_{t+1} = b_{t+1}, y_{d:d+\ell-1}, \theta) = \hat{P}(B_t = k \mid B_{t+1} = b_{t+1}, y_{d:d+\ell-1}, \theta).$$

Also, for  $t = T$  in block  $D$  define

$$\hat{P}(B_t = k \mid B_{d-1} = b_{d-1}, B_{t+1} = b_{t+1}, y_{d:t}, \theta) = \hat{P}(B_T = k \mid B_{d-1} = b_{d-1}, y_{d:t}, \theta).$$

---

**for** iterations  $m = 1, \dots, M$  **do**

1: Update  $\theta^{(m)}$  from  $p(\theta \mid x_{1:T}^{m-1}, y_{1:T})$

2: **for**  $d = 1, \dots, D$  **do**

3:   Define intervals with indices  $B_{\max(1, d-1): \min(d+\ell, T)}$

4:   **for**  $t = d, \dots, d + \ell - 1$  **do** ▷ (Step 1)

5:     **for**  $k = 1, \dots, N$  **do**

6:       calculate  $\hat{P}(B_t = k \mid B_{d-1} = b_{d-1}, y_{d:t}, \theta^{(m)})$

7:   sample  $b'_{d+\ell-1}$  from

$$\{k, \hat{P}(B_{d+\ell-1} = k \mid B_{d+\ell} = b_{d+\ell}, B_{d-1} = b_{d-1}, y_{d:d+\ell-1}, \theta^{(m)})\}_{k=1}^N$$

8:   **for**  $t = d + \ell - 2, \dots, d$  **do**

9:     sample  $b'_t$  from

$$\{k, \hat{P}(B_t = k \mid B_{t+1} = b'_{t+1}, B_{d-1} = b_{d-1}, y_{d:t}, \theta^{(m)})\}_{k=1}^N$$

10:   **for**  $t = d, \dots, d + \ell - 1$  **do** ▷ (Step 2)

11:     sample  $x'_t$  from  $q(x_t \mid B_t = b'_t)$

12:   sample  $u \sim U(0, 1)$

13:   **if**  $u < p(x_{d:d+\ell-1}^{(m-1)}, x'_{d:d+\ell-1} \mid \theta)$  **then** ▷ Equation (C.1)

14:      $x_{d:d+\ell-1}^{(m)} \leftarrow x'_{d:d+\ell-1}$

15:   **else**  $x_{d:d+\ell-1}^{(m)} \leftarrow x_{d:d+\ell-1}^{(i-1)}$

---

# References

- Andrieu, C., Doucet, A., and Holenstein, R. (2010). Particle Markov chain Monte Carlo methods. *Journal of the Royal Statistical Society: Series B (Statistical Methodology)*, 72(3):269–342.
- Andrieu, C. and Roberts, G. O. (2009). The Pseudo-Marginal Approach for Efficient Monte Carlo Computations. *Annals of Statistics*, 37(2):697–725.
- Auger-Méthé, M., Field, C., Albertsen, C. M., Derocher, A. E., Lewis, M. A., Jonsen, I. D., and Mills Flemming, J. (2016). State-space models’ dirty little secrets: even simple linear Gaussian models can have estimation problems. *Scientific Reports*, 6(1):26677.
- Beaumont, M. A. (2003). Estimation of Population Growth or Decline in Genetically Monitored Populations. *Genetics*, 164(3):1139–1160.
- Borowska, A. and King, R. (2023). Semi-complete data augmentation for efficient state-space model fitting. *Journal of Computational and Graphical Statistics*, in press.
- Brooks, S. P. and Gelman, A. (1998). General Methods for Monitoring Convergence of Iterative Simulations. *Journal of Computational and Graphical Statistics*, 7(4):434–455.
- Buckland, S. T., Newman, K. B., Thomas, L., and Koesters, N. B. (2004). State-space models for the dynamics of wild animal populations. *Ecological Modelling*, 171(1):157–175.
- Bucy, R. S. and Senne, K. D. (1971). Digital synthesis of non-linear filters. *Automatica*, 7(3):287–298.
- Cappé, O., Moulines, E., and Rydén, T. (2005). *Inference in Hidden Markov Models*. Springer Verlag, New York.
- Carter, C. K. and Kohn, R. (1994). On Gibbs Sampling for State Space Models. *Biometrika*, 81(3):541–553.
- Chopin, N. and Singh, S. S. (2015). On particle Gibbs sampling. *Bernoulli*, 21(3):1855–1883.
- de Valpine, P. and Hastings, A. (2002). Fitting population models incorporating process noise and observation error. *Ecological Monographs*, 72(1):57–76.
- Deligiannidis, G., Doucet, A., and Pitt, M. K. (2018). The correlated pseudomarginal method. *Journal of the Royal Statistical Society: Series B (Statistical Methodology)*, 80(5):839–870.
- Durbin, J. and Koopman, S. J. (2012). *Time Series Analysis by State Space Methods: Second Edition*. Oxford University Press.

- Fearnhead, P. (2011). MCMC for State-Space Models. In *Handbook of Markov Chain Monte Carlo*, pages 513–529. Chapman & Hall/CRC.
- Fearnhead, P. and Meligkotsidou, L. (2016). Augmentation schemes for particle MCMC. *Statistics and Computing*, 26(6):1293–1306.
- Finke, A., Doucet, A., and Johansen, A. (2016). On embedded hidden Markov models and particle Markov chain Monte Carlo methods. *arXiv*. <https://doi.org/10.48550/arXiv.1610.08962>.
- Frühwirth-Schnatter, S. (2004). Efficient Bayesian parameter estimation. In *State Space and Unobserved Component Models: Theory and Applications*, pages 123–151. Cambridge University Press.
- Gelman, A. and Rubin, D. B. (1992). Inference from Iterative Simulation Using Multiple Sequences. *Statistical Science*, 7(4):457–472.
- Giordani, P. and Kohn, R. (2010). Adaptive Independent Metropolis—Hastings by Fast Estimation of Mixtures of Normals. *Journal of Computational and Graphical Statistics*, 19(2):243–259.
- Haario, H., Saksman, E., and Tamminen, J. (1999). Adaptive proposal distribution for random walk Metropolis algorithm. *Computational Statistics*, 14(3):375–395.
- Herliansyah, R., King, R., and King, S. E. (2022). Laplace approximations for individual heterogeneity capture-recapture models. *Journal of Agricultural, Biological, and Environmental Statistics*, 22(1):401–418.
- Hobert, J. P. (2011). The Data Augmentation Algorithm: Theory and Methodology. In *Handbook of Markov Chain Monte Carlo*, pages 253–293. Chapman & Hall/CRC.
- Julier, S. J. and Uhlmann, J. K. (1997). New extension of the Kalman filter to nonlinear systems. In *Signal Processing, Sensor Fusion, and Target Recognition VI*, pages 182–193.
- Kalman, R. E. (1960). A New Approach to Linear Filtering and Prediction Problems. *Journal of Basic Engineering*, 82(1):35–45.
- Kantas, N., Doucet, A., Singh, S. S., Maciejowski, J., and Chopin, N. (2015). On Particle Methods for Parameter Estimation in State-Space Models. *Statistical Science*, 30(3):328–351.
- King, R. (2011). Statistical ecology. In *Handbook of Markov Chain Monte Carlo*, pages 419–447. Chapman & Hall/CRC.
- King, R. (2012). A review of bayesian state-space modelling of capture-recapture-recovery data. *Interface Focus*, 2(2):190–204.

- Kitagawa, G. (1987). Non-Gaussian State-Space Modeling of Nonstationary Time Series. *Journal of the American Statistical Association*, 82(400):1032–1041.
- Koopman, S. J. and Bos, C. S. (2004). State Space Models with a Common Stochastic Variance. *Journal of Business & Economic Statistics*, 22(3):346–357.
- Koyama, S., Pérez-Bolde, L., Shalizi, C., and Kass, R. (2010). Approximate Methods for State-Space Models. *Journal of the American Statistical Association*, 105(489):170–180.
- Kristensen, K., Nielsen, A., Berg, C. W., Skaug, H., and Bell, B. M. (2016). TMB: Automatic Differentiation and Laplace Approximation. *Journal of Statistical Software*, 70(5):1–21.
- Langrock, R. and King, R. (2013). Maximum likelihood estimation of mark-recapture-recovery models in the presence of continuous covariates. *The Annals of Applied Statistics*, 7(3):1709–1732.
- Langrock, R., MacDonald, I. L., and Zucchini, W. (2012). Some nonstandard stochastic volatility models and their estimation using structured hidden Markov models. *Journal of Empirical Finance*, 19(1):147–161.
- Li, T., Sattar, T. P., and Sun, S. (2012). Deterministic resampling: Unbiased sampling to avoid sample impoverishment in particle filters. *Signal Processing*, 92(7):1637–1645.
- Lin, A., Zhang, Y., Heng, J., Allsop, S. A., Tye, K. M., Jacob, P. E., and Ba, D. (2019). Clustering Time Series with Nonlinear Dynamics: A Bayesian Non-Parametric and Particle-Based Approach. In *Proceedings of the Twenty-Second International Conference on Artificial Intelligence and Statistics*, pages 2476–2484.
- Lindsten, F., Jordan, M. I., and Schön, T. B. (2014). Particle Gibbs with Ancestor Sampling. *Journal of Machine Learning Research*, 15(63):2145–2184.
- Lindsten, F., Schön, T. B., and Jordan, M. (2012). On the use of backward simulation in the particle gibbs sampler. In *2012 IEEE International Conference on Acoustics, Speech and Signal Processing*, pages 3845–3848.
- Meent, J.-W., Yang, H., Mansinghka, V., and Wood, F. (2015). Particle Gibbs with Ancestor Sampling for Probabilistic Programs. In *Proceedings of the Eighteenth International Conference on Artificial Intelligence and Statistics*, pages 986–994.
- Murphy, J. and Godsill, S. J. (2016). Blocked Particle Gibbs Schemes for High Dimensional Interacting Systems. *IEEE Journal of Selected Topics in Signal Processing*, 10(2):328–342.
- Neal, R. M. (2003). Markov Chain Sampling for Non-linear State Space Models Using Embedded Hidden Markov Models. *arXiv*. <https://doi.org/10.48550/arXiv.math/0305039>.

- Newman, K. B., Buckland, S. T., Morgan, B. J. T., King, R., Borchers, D. L., Cole, D. J., Besbeas, P., Gimenez, O., and Thomas, L. (2014). *Modelling Population Dynamics: Model Formulation, Fitting and Assessment using State-space Methods*. Springer.
- Newman, K. B., King, R., Elvira, V., de Valpine, P., McCrea, R. S., and Morgan, B. J. T. (2022). State-space models for ecological time series data: Practical model-fitting. *Methods in Ecology and Evolution*, 14(1):26 – 42.
- Nonejad, N. (2015). Particle Gibbs with ancestor sampling for stochastic volatility models with: heavy tails, in mean effects, leverage, serial dependence and structural breaks. *Studies in Nonlinear Dynamics & Econometrics*, 19(5):561–584.
- Patterson, T. A., Thomas, L., Wilcox, C., Ovaskainen, O., and Matthiopoulos, J. (2008). State-space models of individual animal movement. *Trends in Ecology & Evolution*, 23(2):87–94.
- Rabiner, L. (1989). A tutorial on hidden Markov models and selected applications in speech recognition. *Proceedings of the IEEE*, 77(2):257–286.
- Rainforth, T., Naesseth, C. A., Lindsten, F., Paige, B., van de Meent, J.-W., Doucet, A., and Wood, F. (2016). Interacting Particle Markov Chain Monte Carlo. In *Proceedings of the 33rd International Conference on Machine Learning*, pages 2616–2625.
- Shephard, N. and Pitt, M. K. (1997). Likelihood Analysis of Non-Gaussian Measurement Time Series. *Biometrika*, 84(3):653–667.
- Shestopaloff, A. Y. and Neal, R. M. (2013). MCMC for non-linear state space models using ensembles of latent sequences. *arXiv*. <https://doi.org/10.48550/arXiv.1305.0320>.
- Shestopaloff, A. Y. and Neal, R. M. (2018). Sampling Latent States for High-Dimensional Non-Linear State Space Models with the Embedded HMM Method. *Bayesian Analysis*, 13(3):797–822.
- Smith, A. C. and Brown, E. N. (2003). Estimating a state-space model from point process observations. *Neural Computation*, 15(5):965–991.
- Tanner, M. A. and Wong, W. H. (1987). The Calculation of Posterior Distributions by Data Augmentation. *Journal of the American Statistical Association*, 82(398):528–540.
- Thygesen, U. H., Albertsen, C. M., Berg, C. W., Kristensen, K., and Nielsen, A. (2017). Validation of ecological state space models using the Laplace approximation. *Environmental and Ecological Statistics*, 24(2):317–339.
- Wan, E. A. and Van Der Merwe, R. (2000). The unscented kalman filter for nonlinear estimation. In *Proceedings of the IEEE 2000 Adaptive Systems for Signal Processing, Communications, and Control Symposium*, pages 153–158.



- Wang, X., Li, T., Sun, S., and Corchado Rodríguez, J. (2017). A Survey of Recent Advances in Particle Filters and Remaining Challenges for Multitarget Tracking. *Sensors*, 17(12):2707.
- Wood, S. N. (2010). Statistical inference for noisy nonlinear ecological dynamic systems. *Nature*, 466(7310):1102–1104.